A&A manuscript no.
(will be inserted by hand later)

Your thesaurus codes are:
10.15.2; 10.19.1; 11.09.1; 11.19.2; 11.19.4; 11.19.6

ASTRONOMY AND ASTROPHYSICS
October 24, 2000

A Gould-Belt-like structure in M 83 ⋆

F. Comerón

European Southern Observatory, Karl-Schwarzschild-Str.2, D-85748 Garching bei München, Germany
email: fcomeron@eso.org

Received; accepted

Abstract. VLT archive observations of M 83 are used to study a complex in the disk of that galaxy that shows a remarkable similarity with the Gould Belt. The complex stands out clearly separated from the grand-design spiral pattern of the galaxy, it is several hundred parsecs across, and is resolved into several tens of point sources, thus looking much as the Gould Belt should if observed from above the galactic plane. The point sources are likely to be bright, Trapezium-like clusters, or compact OB associations. Many of them display Hα emission, whose luminosity is estimated to be of the order of that of the Orion nebula. The integrated absolute B magnitude of this complex and the Gould Belt are found to be comparable. The blue colors of some of the members, the abundance of Hα emission, and the lack of any apparent distortion of the shape of the complex due to galactic shear all argue for a very young age.

The similarity in size, location with respect to the spiral pattern of the host galaxy, contents, age, and overall luminosity of the M 83 complex studied here strongly argue for a close relationship between the nature of both structures.

Key words: Galaxy: open clusters and associations (Gould Belt); solar neighbourhood; Galaxies: individual (M 83); spiral; star clusters; structure

1. Introduction

The relationship of the Gould Belt to the structure of the Galaxy has been controversial since its discovery over one and a half century ago (see Stothers & Frogel 1974 and Frogel & Stothers 1977 for a historical review). Some of the main questions regarding the nature of the Gould Belt and the role of similar structures in galactic disks are: what is the relationship, if any, between our local Gould Belt and the large star forming complexes observed elsewhere in ours and other galaxies (Efremov 1995)? Was the formation of the Gould Belt triggered by the passage by a spiral arm, or is it rather the result of a different process? Are Gould-Belt-like structures common in ours and other galaxies, and what is their role in the overall star formation processes in galactic disks?

Much of the uncertainty in the answers to these questions stems from the lack of a precise definition of what the Gould Belt is. This is in turn due to the fact that some definitory features of the Gould Belt, such as the tilt of its midplane and its kinematical peculiarities are visible only from our vantage point inside it. It is unclear if those features are necessary consequences of the formation of Gould-Belt-like complexes, or if such structures may form by essentially identical processes but without displaying some of these distinctive characteristics.

To understand the role of such complexes in galactic disks, it is an urgent task to enlarge the sample of only one such object unequivocally identified so far. This paper calls the attention on a very good candidate found in the disk of the nearby galaxy M 83 sharing many properties with our local Gould Belt. It thus seems a very well suited object for detailed follow-up study aiming at establishing the features of such star forming complexes, a necessary step to understand their origin, evolution, and relationship to galactic structure.

In Section 2 I present the basic data and analysis of the observations on which the discussion of this structure is based. The M 83 complex and its comparison to the local Gould Belt are discussed in Section 3. Concluding remarks are presented in Section 4.

2. Observations and data reduction

The observations used here were obtained on 9 and 11 March 1999 during commissioning of the camera and spectrograph FORS1 at Unit Telescope 1 of the Very Large Telescope (VLT). The data set consists of frames in the B, R, I, and Hα filters of 10, 3, 3, and 15 minutes of exposure time respectively. An image made from these observations is reproduced in Figure 1. Flat fielding of the B, R, and I frames was performed using twilight sky frames taken

Send offprint requests to: F. Comerón

⋆ Based on archive observations collected with the ESO Very Large Telescope.

Fig. 1. A FORS1 image of the field of M 83, measuring $6'8 \times 6'8$. This image is composed of frames taken in the B, R, and I filters. The outlined area highlights the candidate Gould-Belt-like structure discussed in this paper.

between 8 and 13 March. For Hα, the nearest flat fields were obtained more than two weeks after the observations and were not appropriated due to a rapidly evolving contamination of the detector at the time. Much better results were obtained by ratioing the Hα frame by the flat field in R, taken the day before.

Object detection and instrumental photometry were carried out on each frame using DAOPHOT (Stetson 1987). The parameters of the point spread function (PSF) derived from a bright, isolated point source were used to detect point and small extended sources using DAOFIND, and PSF-fitting photometry was then performed using the task PEAK. A magnitude cutoff was set on the detected sources by visual inspection of the images according to the level where spurious detections began to appear.

Since accurate flux calibration was not a high priority during instrument commissioning, no photometric standards were observed simultaneously with the observations of M 83. To approximately calibrate the B, R, and I images, I have first taken instrumental zeropoints determined on 13-15 December 1998, given in the Paranal Observatory FORS1 webpages. Then, I recalculated them with observations of standards in the field of PG1323-086 (Landolt 1992), observed in late March 1999. The comparison shows differences of -0.28 mag in B (March 1999 minus December 1998), -0.20 mag in R, and -0.22 mag in I. The values adopted here asume a linear variation of the zeropoint as if it were due to a slow evolution of the throughput. No variation is assumed in the extinction coefficients, for which I have adopted the December 1998 values. Obviously, this procedure does not take into account possible differences in the transparency conditions of each night. Meteorological data for Paranal on the nights when either the standard stars or M 83 were observed, available through the VLT archive webpages, do not suggest conditions significantly below the average, but part of the measured difference in zeropoints may be indeed due to transparency variations. Therefore, the magnitude calibration used here should be taken with caution: a rather pessimistic estimate suggests that systematic errors at each band may be as high as 0.2 mag, although errors in color should be considerably smaller, certainly below 0.1 mag.

As no narrow-band images of the continuum adjacent to Hα are available, it is not possible to measure the Hα

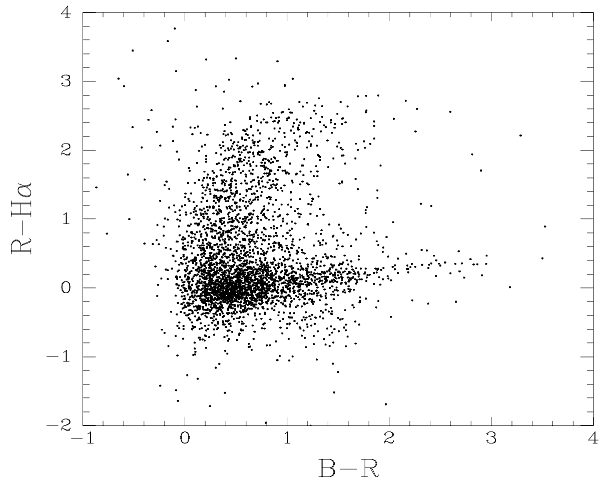

Fig. 2. $(B-R)$, $(R-m_{\mathrm{H}\alpha})$ diagram showing the position of sources with and without Hα emission. The zeropoint of the $(R-m_{\mathrm{H}\alpha})$ color has been set so as to coincide with the centroid of the cluster of sources at the lower left of the distribution of points.

flux from photometry on continuum-subtracted images. However, HII regions can be identified and their fluxes roughly estimated by using the R image as a reference of the continuum contribution to the flux. Let us assume that line and continuum fluxes are related to the magnitudes in the R and Hα filters, m_R and $m_{\mathrm{H}\alpha}$, by:

$$R = C - 2.5\log(f_R + \frac{F_{\mathrm{H}\alpha}}{W_R}) \quad (1a)$$

$$m_{\mathrm{H}\alpha} = C - 2.5\log(f_R + \frac{F_{\mathrm{H}\alpha}}{W_{\mathrm{H}\alpha}}) \quad (1b)$$

where $10^{0.4C}$ is the flux per unit wavelength in erg s^{-1} cm^{-2} Å^{-1} of a zero-magnitude star, f_R is the continuum flux per unit wavelength in the same units, $F_{\mathrm{H}\alpha}$ is the flux from the HII region in erg s^{-1} cm^{-2}, and W_R, $W_{\mathrm{H}\alpha}$ are the passband widths of the R and Hα filters respectively, in Å. The Hα flux can thus be estimated from

$$F_{\mathrm{H}\alpha} = \frac{W_{\mathrm{H}\alpha}W_R}{W_R - W_{\mathrm{H}\alpha}} \times 10^{0.4C} \times (10^{-0.4m_{\mathrm{H}\alpha}} - 10^{-0.4R}) \quad (2)$$

Adopting $W_{\mathrm{H}\alpha} = 61$ Å, $W_R = 1500$ Å from the FORS1 Users Manual and $C = -21.62$ from the absolute flux calibration of the R magnitude (Bessell 1979),

$$F_{\mathrm{H}\alpha}(\mathrm{erg\ s^{-1}cm^{-2}}) = 1.43 \times 10^{-7}(10^{-0.4m_{\mathrm{H}\alpha}} - 10^{-0.4R}) \quad (3)$$

It must be stressed that this is a crude estimate forced by the unavailability of more suitable material for flux measurements. Moreover, $m_{\mathrm{H}\alpha}$ is computed by treating each source as unresolved, while extended Hα emission is clearly seen in the Hα image. An additional approximation comes from unavailability of zeropoints in the Hα filter: $m_{\mathrm{H}\alpha}$ is approximately calibrated by assuming that most detected point sources are not HII regions, have a continuum with no strong features in R, and thus have $R - m_{\mathrm{H}\alpha} \simeq 0.0$. The assumption seems justified *a posteriori* by Fig. 2, showing the distribution of point sources in the $B-R$, $R-m_{\mathrm{H}\alpha}$ diagram. Most sources clump at blue-to-moderately red $B-R$ within a narrow range of $R-m_{\mathrm{H}\alpha}$, as expected from sources with little extinction and no Hα emission and foreground stars in the field. A branch extends to redder $B-R$ while keeping a near-zero $R-m_{\mathrm{H}\alpha}$; these could be old clusters, supergiant stars, highly reddened sources of M 83, or foreground late-type stars. Finally, HII regions of M 83 occupy the area with larger $R-m_{\mathrm{H}\alpha}$. As expected, $B-R$ and $R-m_{\mathrm{H}\alpha}$ are correlated due to the contribution of Hα to the broad-band R flux.

3. Results and discussion

Figure 1 shows M 83 as a grand-design two-armed SABc barred spiral (Tully 1988) with many star forming complexes along its arms. Global properties of these complexes have been studied by Larsen & Richtler 1992. The same distance to M 83 as used by these authors, 3.7 Mpc, is adopted here. Note however that a wide range of distances can be found in the literature, ranging from the quoted value up to 8.9 Mpc (Sandage & Tammann 1987), implying a distance modulus almost two magnitudes larger, absolute magnitudes correspondingly brighter, and sizes 2.4 times larger.

A remarkable feature is the conspicuous, isolated complex in the Southeastern quadrant of Figure 1. This complex, shown in more detail in Figure 3, has an approximate size of $\sim$ 25", corresponding to $\sim$ 450 pc at the adopted distance of M 83, well above the typical sizes of OB associations (e.g. de Zeeuw 1999) and individual giant molecular clouds (Blitz & Williams 1999). Nevertheless, this size is similar to the estimated extent of the Gould Belt (e.g. Pöppel 1997). The qualitative agreement is even better if greater distances, as quoted above, are adopted.

Another characteristic shared between the M 83 complex and the Gould Belt seems to be the detachment from the spiral structure of the host galaxy. Tracers of spiral structure in the solar neighbourhood delineate three major arm fragments probably related through an overall four-armed pattern (Vallée 1995, Amaral & Lépine 1997, Russeil 1998, Englmaier & Gerhard 1999). The Sun lies approximately halfway between two arms, implying that the last passage of the solar neighbourhood by one of them took place at a time $t \simeq \pi/4(\Omega - \Omega_p)$ in the past, where Ω is the local value of the angular rotation curve of the Galaxy and Ω_p is the angular speed of the spiral pattern. Recent observations (Amaral & Lépine 1997, Mishurov et al. 1997) favor values of Ω_p close to Ω, implying $t \sim 10^8$ yr

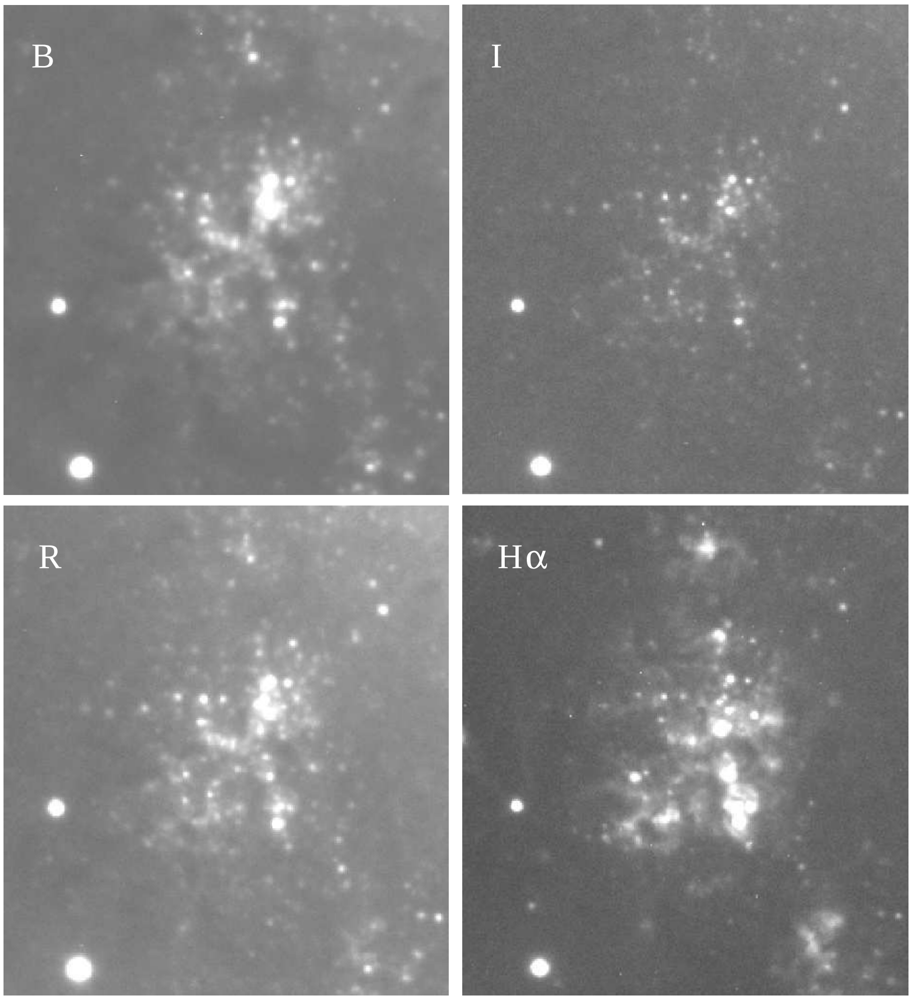

Fig. 3. An enlarged view of the area outlined in Figure 1 in the different available filters.

or larger. This leaves the Gould Belt, whose age is estimated at $\sim$ 30 Myr (Lindblad et al. 1997, Torra et al. 2000), and possibly other features such as the Cygnus arm (Odenwald & Schwartz 1993) as large structures not directly related to the grand-design spiral pattern of the Milky Way. This is also the case of the M 83 complex, whose detachment from the spiral structure is even more obvious in wider field images of M 83 that show the arm extending out of the upper left edge of Figure 1 streaming until past its azimuthal position (e.g. Immler et al. 1999).

Table 1 lists the brigthtest point sources in the B image of the complex ($B < 22$, or $M_B < -5.84$; positions are given in Figure 4). The brigthest source has $M_B = -8.1$, similar to that of bright, Trapezium-like galactic clusters (Battinelli et al. 1994). Brighter point sources, perhaps similar to luminous galactic compact OB associations such as Cygnus OB2 (Knödlseder 2000) or NGC 3603 (Moffat et al. 1994) are seen elsewhere in the disk of M 83 (Larsen & Richtler 1992, but not in the complex under discussion. Hα luminosities of the brightest HII regions in the M 83 complex are also of the order of that of the Orion nebula, $\sim 10^{37}$ erg s^{-1} (Kennicutt 1984), while their $L_{\mathrm{H}\alpha}$ vs. M_B fits well with the low luminosity end of the relationship found by Bresolin & Kennicutt 1997 for giant HII regions in spiral galaxies. Such match supports the validity of the method used here to estimate the Hα luminosity.

It is also possible to compare the integrated B-band luminosities of the M 83 complex the Gould Belt. For the former, one measures $M_B = -11.4$ by adding up the flux over the area of the complex and subtracting the background contribution evaluated from the surrounding area. For the Gould Belt, an estimate is obtained by approximating the bulk of the blue luminosity by the contribution of its early-type stars. A list of early-type stars up to 600 pc from the Sun, the approximate radius of the Gould Belt, has been taken from the *Hipparcos* catalog (Perryman et al. 1997). The absolute B magnitude of each star is derived from the spectral type using the absolute magnitude and intrinsic color calibrations of Schmidt-Kaler 1982. Neither the parallax or the photometric information in the *Hipparcos* catalog are used for this purpose, thus precluding the appearance of biases in the magnitudes due to the non-Gaussianity of the error in distance for a Gaussian error distribution in parallaxes.

Table 1. Brightest point sources in the M 83 star forming complex

Number	R.A. (2000)	Decl. (2000)	B	$(B-R)$	$(R-I)$	$\log L_{\mathrm{H}\alpha}$ erg s^{-1}
1	13 37 06.75	-29 54 42.5	21.7	0.18	-0.32	
2	13 37 06.95	-29 54 29.4	21.5	0.20		36.2
3	13 37 06.95	-29 54 22.1	22.0	0.08		
4	13 37 06.98	-29 54 34.3	21.3	0.30	-0.29	36.0
5	13 37 07.03	-29 54 29.1	21.5	0.30		36.2
6	13 37 07.06	-29 54 24.6	21.6	0.20	0.16	
7	13 37 07.13	-29 54 29.0	21.9	0.42		36.6
8	13 37 07.15	-29 54 20.4	21.1	0.51	-0.14	35.4
9	13 37 07.17	-29 54 38.9	21.2	0.57	-0.88	36.7
10	13 37 07.20	-29 54 24.9	20.4	0.35	0.12	
11	13 37 07.24	-29 54 27.7	21.0	0.32	-0.28	
12	13 37 07.24	-29 54 30.0	21.4	0.26	-0.48	35.8
13	13 37 07.26	-29 54 38.7	20.7	0.53	-0.46	36.3
14	13 37 07.29	-29 54 40.7	20.2	0.87	-0.16	36.7
15	13 37 07.34	-29 54 24.8	19.7	0.61	-0.04	36.5
16	13 37 07.34	-29 54 35.3	21.5	1.11	-1.03	37.0
17	13 37 07.35	-29 54 28.2	19.9	0.33	-0.01	
18	13 37 07.40	-29 54 26.9	19.8	-0.06	-0.40	
19	13 37 07.43	-29 54 21.5	21.4	0.43	-0.10	35.9
20	13 37 07.47	-29 54 25.9	21.3	-0.21	-0.35	
21	13 37 07.47	-29 54 23.5	21.6	0.06	-0.59	35.6
22	13 37 07.48	-29 54 29.2	21.5	0.40		35.9
23	13 37 07.52	-29 54 31.5	21.8	0.51	-0.09	
24	13 37 07.53	-29 54 25.7	21.0	-0.24	0.26	
25	13 37 07.57	-29 54 32.6	21.8	0.34	-0.15	
26	13 37 07.61	-29 54 38.9	21.9	0.63	-0.08	35.3
27	13 37 07.66	-29 54 32.0	20.8	0.15	-0.50	36.2
28	13 37 07.75	-29 54 31.8	21.2	0.58	0.14	
29	13 37 07.79	-29 54 31.1	21.2	0.32	-0.30	
30	13 37 07.80	-29 54 39.9	21.5	0.46	-0.70	36.1
31	13 37 07.81	-29 54 36.1	21.4	0.29	-0.29	
32	13 37 07.86	-29 54 31.1	21.0	0.29	-0.24	
33	13 37 07.86	-29 54 37.4	22.0	1.16	0.09	
34	13 37 07.88	-29 54 27.8	21.4	0.24	-0.48	
35	13 37 07.91	-29 54 26.9	21.1	0.99	0.04	35.6
36	13 37 07.94	-29 54 29.3	20.8	0.47	-0.13	
37	13 37 08.06	-29 54 35.3	20.9	0.15	-0.21	35.7
38	13 37 08.09	-29 54 38.1	22.0	1.03	-0.15	35.8
39	13 37 08.14	-29 54 26.5	21.0	0.25	-0.16	
40	13 37 08.15	-29 54 35.8	21.5	0.42	-0.92	36.5

The Gould Belt is thus estimated to have $M_B = -12.7$. This is an approximation to the integrated magnitude that the Gould Belt would have if observed from a vantage point similar to that from which the M 83 complex is seen, which minimizes the extinction. The approach outlined above ignores a number of complications, such as the contribution of fainter stars, possible errors in the spectral type vs. absolute magnitude calibration, progressive incompleteness of the catalog with increasing distance, and large relative uncertainties in the parallax at the sample horizon adopted here, thus including or excluding stars from the census due to errors in the parallax. Given the difficulty in evaluating the combined effect of all the uncertaintes, the value above should be taken only as a rough indication. For instance, changing the sample horizon to 400 pc or 750 pc changes the estimated M_B to -12.1 and -13.0 respectively, giving an idea of the uncertainty due to that factor alone.

Table 2 summarizes the global properties of the Gould Belt and the M 83 complex. The distance of the M 83 complex to the center of its host galaxy is considerably smaller than that of the Gould Belt, but it becomes more comparable when the relative sizes of the Milky Way and M 83 are taken into account. The field covered in Figure 1

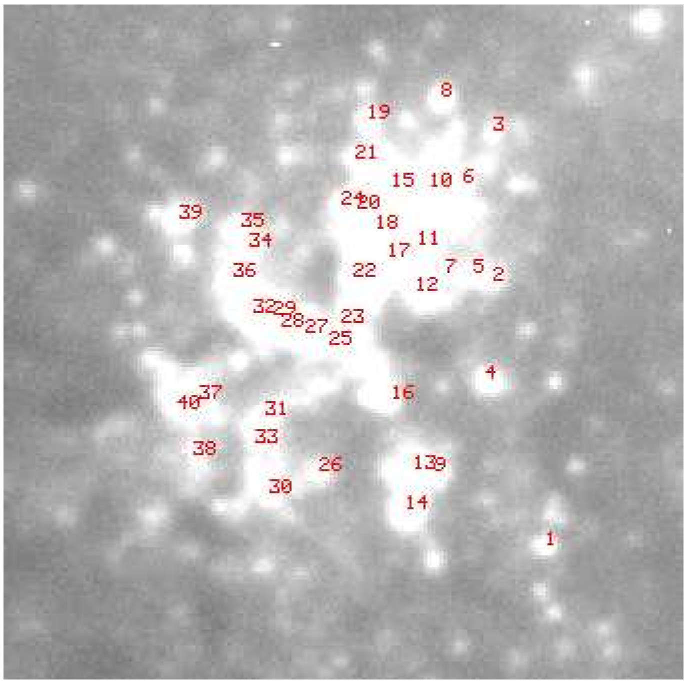

Fig. 4. Finding chart for the sources listed in Table 1, in the B band.

Table 2. Comparison between the global properties of the Gould Belt and the M 83 complex

	M 83 complex	Gould Belt
diameter (pc)[1]	450	600
dist. to center of galaxy (kpc)	3.3	8.5
M_B	-11.4	~ -12.7
age (yr)[2]	$\sim 10^7$	3×10^7 yr

Notes:
[1]: the diameter adopted for the Gould Belt is the distance from the ρ Ophiuchi to the Orion star forming complexes, which approximately delimit its extent in the direction of its maximum tilt. This may be increased to $\sim$ 950 pc if the Monoceros R2 complex (Carpenter et al. 1997) is included as a member of the Gould Belt.
[2]: see references at the beginning of Sect. 3 for the Gould Belt. For the M 83 complex, this is just a crude estimate based on the lack of distortion by shear, as discussed in the text.

is 7.3 kpc in side at the adopted distance of M 83, meaning that the most distant regions from the center of M 83 imaged are a bit more than halfway of the distance of the Sun to the center of the Milky Way. However, if the actual distance is 8.9 Mpc (Sandage & Tammann 1987), the distance of the complex to the center of M 83 becomes 7.9 kpc, practically identical to the distance of the Gould Belt to the center of the Milky Way. Other properties also compare very well with this larger distance: the absolute magnitude of the M 83 complex becomes then -13.4, and the diameter of 1,100 pc is still similar to that of the Gould Belt, especially if the Monoceros complex is included as a member of the latter (see note to Table 2).

The available data do not allow one to precisely date the M 83 complex, but the small $(B-I)$ value of the bluest sources and the abundance of HII regions suggest and age of a few 10^7 years. A better determination may be obtained with UBV photometry using models for the integrated properties of stellar populations as a function of age (e.g. Girardi et al. 1995). The young age is also suggested by the lack of any visible elongation of the complex due to galactic shear. The characteristic timescale of galactic shear may be defined as the time needed by two objects moving in circular orbits around the center of the galaxy, and initially aligned along the galactocentric direction, to move with respect to each other in the perpendicular direction by a length equal to their initial separation. The characteristic shear timescale is thus $\tau \sim (2A)^{-1}$ (where $A = 0.5[V/R - \mathrm{d}V/\mathrm{d}R]$ is the first Oort constant), and can be estimated from the rotation curve of M 83 (de Vaucouleurs et al. 1983). This gives $A \simeq 21$ km s^{-1} kpc^{-1} and $\tau \simeq 2.4 \times 10^7$ years at the position of the M 83 complex, suggesting that its present age is only a fraction of that value.

Existing observations of hot phases of the interstellar medium do not show any prominent features associated to this complex (Ehle et al. 1998, Immler et al. 1999) indicative of recent supernovae. Most high resolution observations of the atomic and molecular interstellar gas of M 83 concern a region of the Eastern arm North of the complex studied here (e.g. Rand et al. 1999 and references therein). However, VLA HI and Fabry-Pérot Hβ observations of the entire disk of M 83 are discussed in detail by Tilanus & Allen (1993). A local minimum in the HI column density near the position of the complex studied here appears at the lowest resolution of their maps, 30". However, the 12"-resolution map shows that the minimum lies actually next to the complex, rather than centered on it. Velocity maps produced from the Hβ observations at 12" resolution do not show any clear systematic radial motions in the complex. However, recent CO observations (Andersson, in prep.) show a bridge of emission between the arms inside and outside the complex with multiple-peaked, high-amplitude radial velocity profiles near, but not quite coincident with, the position of the complex.

4. Concluding remarks

The star forming complex in M 83 is similar to the Gould Belt in size, relative location in the galaxy, contents, luminosity and age. The observations presented in this paper, not having been designed to study this complex, are of limited use to address in more detail the comparison. New observations in the visible and near-infrared may allow the exploration of additional aspects such as age patterns showing the spatial progress of star formation, or the existence of new, embedded star forming sites. On the other hand, detailed observations of different phases of the gas in the complex may check model predictions on the origin of the Gould Belt (e.g. Comerón & Torra 1992) that link it to large-scale disturbances in the HI layer of the Galaxy.

An obvious direction of future work should go into identifying similar structures in other galaxies. In this respect it is remarkable the intriguing similarities in size and location, with equally intriguing differences in contents, found between the complex discussed here and a young complex recenlty studied by Elmegreen et al. 2000 in NGC 6946. This complex is dominated by a very young globular cluster likely to have played an essential role in triggering the formation of the rest of the structure, but such a powerful engine is absent from the M 83 complex and the Gould Belt. The question is therefore open as to whether both kind of structures, with and without central engines, may appear as different outcomes of an essentially identical process, or are rather the result of substantially different star forming mechanisms.

The numerous HII regions of the M 83 complex may also be used as probes of its large-scale kinematics. Kinematical peculiarities in the Gould Belt are well known (see Frogel & Stothers 1977, and Torra et al. 2000 and Lindblad 2000 for recent work), but they seem to affect motions in the galactic plane only. As such, they would be hard to detect in M 83 given our nearly face-on view. However, as noted in Comerón 1999, the maintenance of the tilt of the Gould Belt implies a coherent pattern of motions in the vertical direction. This coherence, and the amplitude of the vertical motion implied by the tilt, should produce noticeable spatial gradients of this component near the galactic plane-crossing epochs. The tilt is one of the most puzzling features of the Gould Belt (and the one that allows us to see it as a distinct entity separated from the backdrop of the Milky Way in the night sky), and a fundamental question on the M 83 complex is whether it is also oscillating around the plane of its host galaxy. While our face-on view prevents us from directly seeing the tilt, its kinematical consequence may appear as a systematic pattern in the radial velocity of the HII regions if the amplitude of the oscillation is similar as for the Gould Belt, and if the M 83 complex is at present noo too far from crossing the plane of M 83. The detection of such a pattern would almost definitely prove the close relationship between the M 83 complex and the Gould Belt, and would bear essential implications concerning the origin of such structures in galatic disks.

Acknowledgements. It is a great pleasure to thank the ESO Archive Group for their efforts in making available such a fine research tool to the astronomical community, to Dr. R. Gilmozzi for obtaining the images that have been used here, and to the commissioning teams of the VLT and FORS for providing such excellent instruments to the astronomical community. I am very pleased to thank Prof. P.O. Lindblad for comments on the manuscript and for drawing to my attention to Elmegreen et al.'s work on NGC 6946, and Dr. A. Andersson for kindly providing CO data prior to publication. The referee, Prof. A. Blaauw, is thanked for comments that improved the readability of this paper.

References

Amaral, L.H., Lépine, J.R.D., 1997, MNRAS, 286, 885.
Battinelli, P., Brandimarti, A., Capuzzo-Dolcetta, R., 1994, A&AS, 104, 379.
Bessell, M.S., 1979, PASP, 91, 589.
Blitz, L., Williams, J.P., 1999, in "The origin of stars and planetary systems", eds. C.J. Lada and N.D. Kylafis, Kluwer Acad. Publ.
Bresolin, F., Kennicutt, R.C., 1997, AJ, 113, 975.
Carpenter, J.M., Meyer, M.R., Dougados, C., Strom, S.E., Hillenbrand, L.A., 1997, AJ, 114, 198.
Comerón, F., 1999, A&A, 351, 506.
Comerón, F., Torra, J., 1992, A&A, 261, 94.
Efremov, Y.N., 1995, AJ, 110, 2757.
Elmegreen, B.G., Efremov, Y.N., Larsen, S., 2000, ApJ, 535, 748.
Ehle, Pietsch, W., Beck, R., Klein, U., 1998, A&A, 329, 39.
Englmaier, P., Gerhard, O., 1999, MNRAS, 304, 512.
Frogel, J.A., Stothers, R., 1977, AJ, 82, 890.
Girardi, L., Chiosi, C., Bertelli, G., Bressan, A., 1995, A&A, 298, 87.
Immler, S., Vogler, A., Ehle, M., Pietsch, W., 1999, A&A, 352, 415.
Kennicutt, R.C., 1984, ApJ, 287, 116.
Knödlseder, J., 2000, A&A, 360, 539.
Landolt, A.U., 1992, AJ, 104, 340.
Larsen, S.S., Richtler, T., 1999, A&A, 345, 59.
Lindblad, P.O., A&A, in press.
Lindblad, P.O., Palous, J., Lodén, K., Lindegren, L., 1997, in Hipparcos Velice'97, ESA SP-402, 507.
Mishurov, Y.N, Zenina, I.A., Dambis, A.K., Mel'nik, A.M., Rastorguev, A.S., 1997, A&A, 323, 775.
Moffat, A.F.J, Drissen, L., Shara, M.M., 1994, ApJ, 436.
Odenwald, S.F., Schwartz, P.R., 1993, ApJ, 405, 706.
Perryman, M.A.C., Lindegren, L., Kovalevsky, J., Hoeg, E., Bastian, U., Bernacca, P.L., Crézé, M., Donati, F., Grenon, M., van Leeuwen, F., van der Marel, H., Mignard, F., Murray, C.A., Le Poole, R.S., Schrijver, H., Turon, C., Arenou, F., Froeschlé, M., Petersen, C.S., 1997, A&A, 323, L49.
Pöppel, W.G.L., 1997, Fund. Cosm. Phys., 18, 1.
Rand, R.J., Lord, S.D., Higdon, J.L., 1999, ApJ, 513, 720.
Russeil, D., 1998, PhD Thesis, Univ. de Provence.
Sandage, A., Tammann, G.A., 1987, "A revised Shapley-Ames Catalog of bright galaxies", Carnegie Inst. of Washington Publ., 2nd ed.
Schmidt-Kaler, T., 1982, in Landolt-Börnstein, Vol. 2b, eds. J. Schaifers and H.H. Voigt, Springer-Verlag.
Stetson, P.B., 1987, PASP, 99, 191.
Stothers, R., Frogel, J.A., 1974, AJ, 79, 456.
Tilanus, R.P.J., Allen, R.J., 1993, A&A, 274, 707.
Torra, J., Fernández, D., Figueras, F., 2000, A&A, 359, 82.
Tully, R.B., 1988, Nearby Galaxies Catalogue, Cambridge Univ. Press.
Vallée, J.P., 1995, ApJ, 454, 119.
de Vaucouleurs, G., Pence, W.D., Davoust, E., 1983, ApJS, 53, 17.
de Zeeuw, P.T., Hoogerwerf, R., de Bruijne, J.H.J., Brown, A.G.A., Blaauw, A., 1999, AJ, 117, 354.